

The Hourglass as seen with HST/WFPC2

J. Maíz Apellániz¹, L. Úbeda², R. H. Barbá³, J. W. MacKenty², J. I. Arias³,
and A. I. Gómez de Castro⁴

¹ Centro de Astrobiología, INTA-CSIC, Spain

² Space Telescope Science Institute, USA

³ Universidad de La Serena, Chile

⁴ Universidad Complutense de Madrid, Spain

Abstract

We present a multi-filter HST/WFPC2 UV-optical study of the Hourglass region in M8. We have extracted the stellar photometry of the sources in the area and obtained the separations and position angles of the Herschel 36 multiple system: for Herschel 36 D we detect a possible orbital motion between 1995 and 2009. We have combined our data with archival IUE spectroscopy and measured the Herschel 36 extinction law, obtaining a different result from that of Cardelli et al. (1989) due to the improvement in the quality of the optical-NIR data, in agreement with the results of Maíz Apellániz et al. (2014). A large fraction of the UV flux around Herschel 36 arises from the Hourglass and not directly from the star itself. In the UV the Hourglass appears to act as a reflection nebula located behind Herschel 36 along the line of sight. Finally, we also detect three new Herbig-Haro objects and the possible anisotropic expansion of the Hourglass Nebula.

1 Motivation

Herschel 36 (O7: V + sec, Sota et al. 2014) is a unique object. It is the main ionizing source of the Hourglass Nebula (for most of M8 it is 9 Sgr), a ZAMS SB3 system (O7.5 V + O9 V + B0.5 V, Arias et al. 2010), and the prototype of large- R_{5495} extinction laws (Cardelli et al. 1989). Herschel 36 C (0'25 away) is another B star companion, deeply embedded in dust (Goto et al 2006 and contribution by J. Maíz Apellániz in these proceedings). In the surrounding nebula, the Hourglass region has a very high surface brightness, the gas and dust distributions are complex (Arias et al. 2006), and several other interesting objects (Goto et al. 2006, Arias et al. 2006) can be found. All of this prompted us to request HST time during Supplemental Cycle 16, which was the last chance for FUV observations with WFPC2.

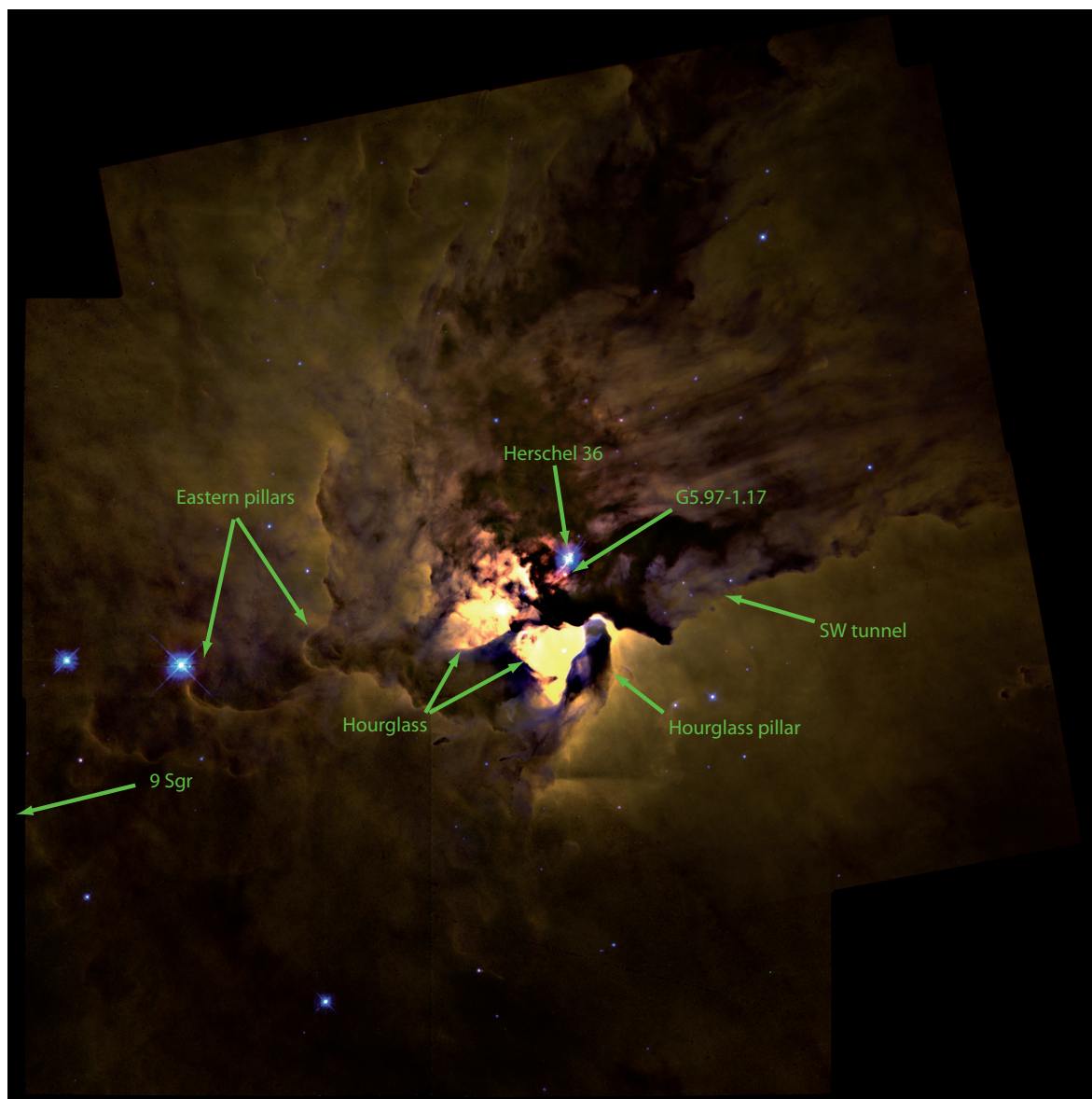


Figure 1: F656N (red) + F487N (green) + F547M (blue) WFPC2 mosaic of the extended region around the Hourglass. Redder regions indicate higher extinction in the nebular lines. In bluish regions scattered radiation is more significant. The field size is $205'' \times 205''$ ($1.3 \text{ pc} \times 1.3 \text{ pc}$) and N is 45° CCW from top.

2 The data

We used three kinds of data:

- Archival WFPC2 data (GO 6227, 1995, PI: Trauger). These have the Hourglass in the PC, with WF2 to the W and include $V + I$ filters (F547M + F814W) and nebular filters (F487N + F502N + F656N + F658N + F953N).
- New WFPC2 data (GO 11 981, 2009, PI: Maíz Apellániz). These have the Hourglass in the PC, with WF2 to the E and include new FUV to B -band filters (F170W + F255W + F336W + F439W), an R -band filter (F675W), and previously used filters for larger coverage and second epochs (F487N + F547M + F656N + F814W).
- Archival 2MASS JHK_s photometry and IUE spectroscopy for Herschel 36.

3 Processing

See Arias et al. (2006) for the initial processing of GO 6227 data. We performed aperture photometry for point-like or quasi-point-like sources using the original (geometrically-distorted) data and selecting the best exposure time as a function of magnitude. For saturated sources we applied techniques similar to that of Gilliland (1994) for GAIN=15 and Maíz Apellániz (2003) for GAIN=7. We used a realistic (spatially-varying) background subtraction and applied CTI, contamination, and aperture corrections. Aperture and zero-point uncertainties were added to the final result. A ghost produced by Herschel 36 was discarded in the long exposures. Finally, the nebulosity was analyzed with large-area photometry.

4 The overall structure of M8

As seen in Figure 1, the Hourglass has a much higher surface brightness than the rest of M8. The eastern pillars point towards 9 Sgr (O4 V((f))z, Sota et al. 2014), the main ionizing source of M8. The southern limit of the Hourglass is a pillar pointing towards Herschel 36. The region around Herschel 36 shows higher extinctions than the Hourglass (Figure 1 and Arias et al. 2006): reddened holes are seen among (even more extinguished) dark regions. Some regions (tunnel towards the SW, part of the Hourglass pillar) are relatively brighter in F547M with respect to F656N or F487N: they are illuminated by mostly non-ionizing radiation.

5 Herschel 36 and its reflection nebula

Herschel 36 is the only bright point source in the FUV (Figure 2), but surprisingly it contains only $29 \pm 6\%$ of the F170W flux in the PC. Furthermore, there is only partial



Figure 2: F439W (red) + F336W (green) + F170W (blue) PC mosaic of the Hourglass. Herschel 36 is the bright point source in the upper right quadrant. The extended F439W and F336W is mostly of nebular origin while F170W is mostly reflected light. The field size is $34'' \times 34''$ ($0.22 \text{ pc} \times 0.22 \text{ pc}$) and N is 45° CCW from top.

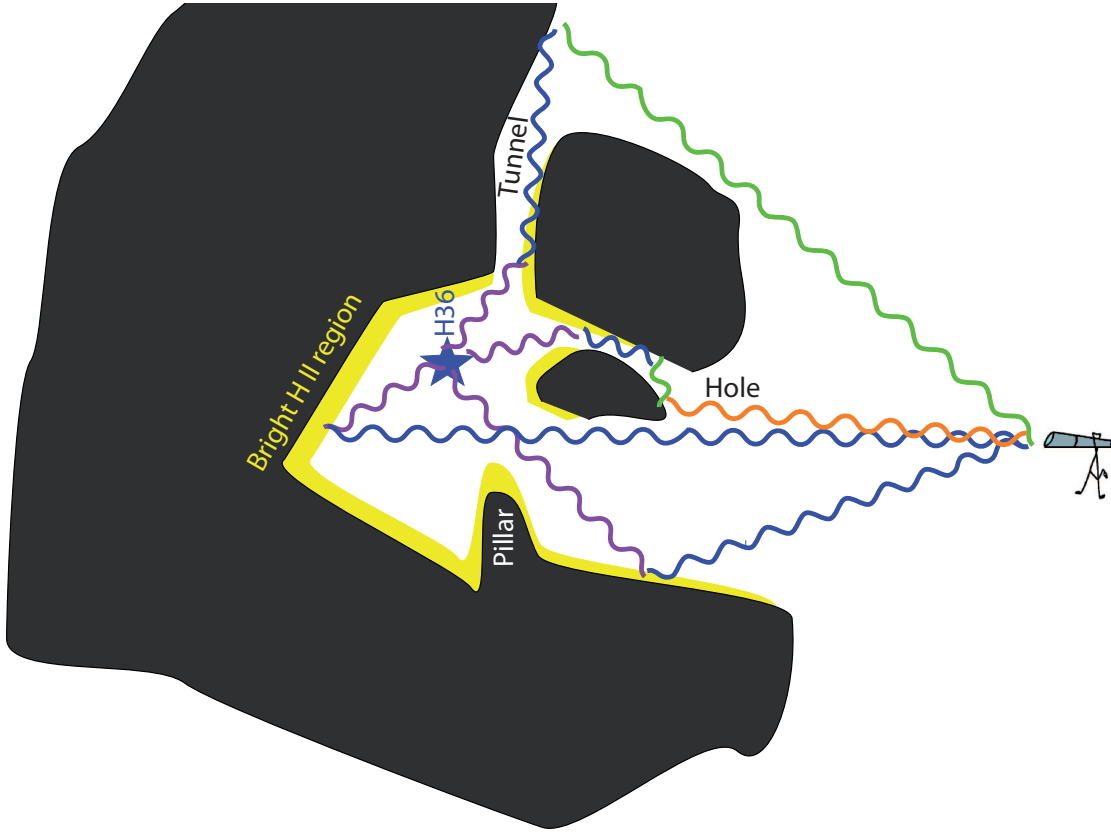


Figure 3: A toy model of the Hourglass region in M8 seen in cross section with respect to the plane of the sky. The path followed by radiation is represented by progressively redder lines as it is scattered in different parts of the nebula. The telescope position marks the direction of our point of view. The effect of external ionizing sources such as 9 Sgr is not included.

Table 1: Results of the CHORIZOS fits for Herschel 36.

Quantity	CCM laws	New laws
χ_{red}^2	5.3	2.0
$E(4405 - 5495)$	0.883 ± 0.008	0.784 ± 0.008
R_{5495}	5.098 ± 0.073	5.942 ± 0.096
$\log d^*$	3.049 ± 0.007	3.023 ± 0.007
$E(\text{F}439\text{W} - \text{F}547\text{M})$	0.954 ± 0.008	0.835 ± 0.008
$A_{\text{F}547\text{M}}$	4.512 ± 0.037	4.670 ± 0.038
$\text{F}547\text{M}_0$	5.743 ± 0.033	5.613 ± 0.035

* Do not trust: it assumes a single, typical MS star.

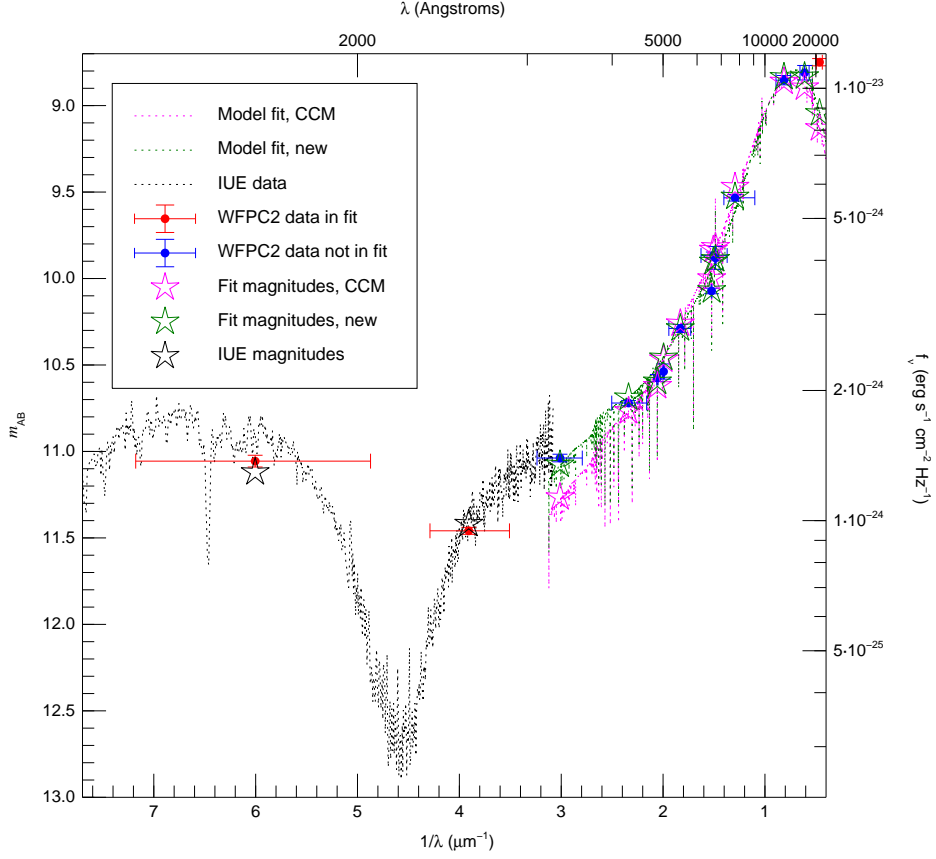


Figure 4: WFPC2+2MASS photometry, CHORIZOS fits to the optical+NIR photometry using the CCM and new families of extinction laws, and IUE spectroscopy of Herschel 36. The synthetic magnitudes are also shown for the two fits and the IUE spectroscopy. Note that the new extinction laws provide a better fit than the CCM ones.

correlation between nebular emission and diffuse F170W (indicating that the cause is not the red leak). The latter comes preferentially from the more extinguished regions: holes around Herschel 36 and NW part of the Hourglass. The preferred explanation is that the FUV diffuse radiation is mostly (forward) scattered light (with smaller contributions from other sources such as free-free, free-bound, and 2-photon Lyman α continuum). Our proposed geometry is shown in Figure 3:

- Herschel 36 is creating a cavity inside the molecular cloud.
- The direct light from the star arrives at us through a partially open hole.
- The bright regions of the Hourglass are farther away than Herschel 36 and they are the visible surface of the molecular cloud directly illuminated by the star.

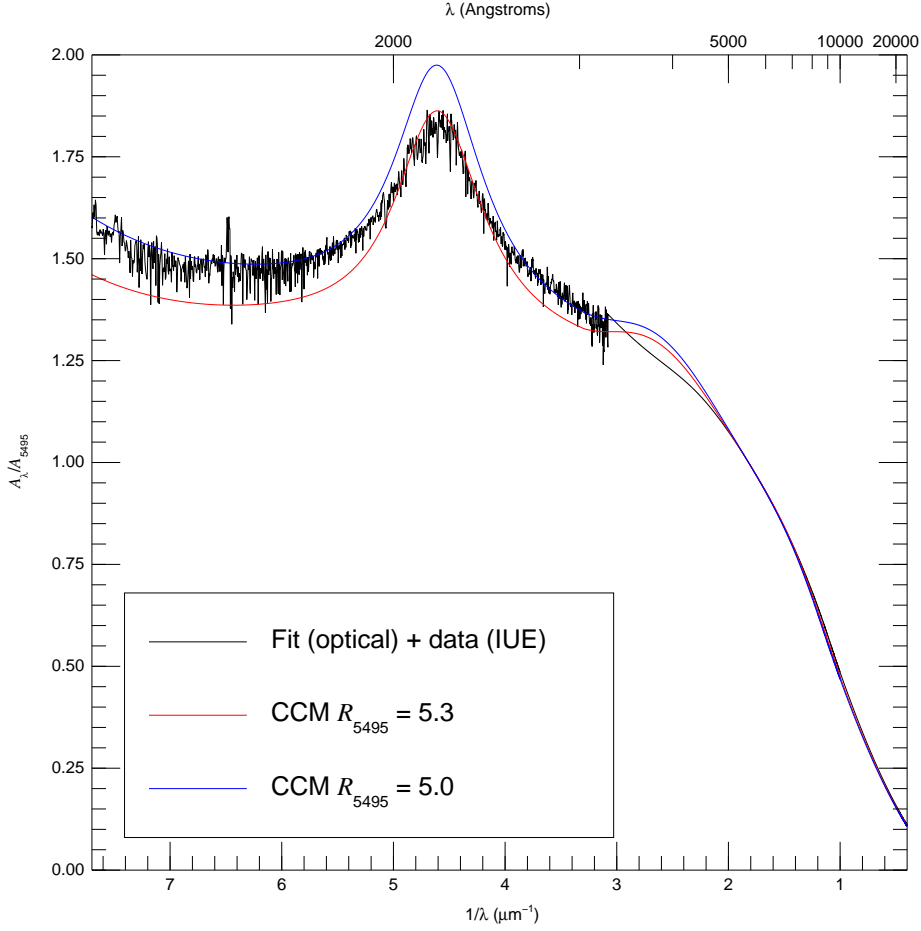


Figure 5: The Herschel 36 extinction law. The optical+NIR part is a CHORIZOS fit to the WFPC2 data using the new family of extinction laws. The UV part is derived from the IUE data and the TLUSTY intrinsic SED obtained with CHORIZOS. Two CCM extinction laws are shown for comparison.

- The cloud is porous e.g. SW tunnel.

6 Herschel 36: optical+NIR analysis

We used CHORIZOS (Maíz Apellániz 2004, 2013b) to measure the Herschel 36 extinction. We fixed the luminosity class (5.0) and T_{eff} (38400 K). We left the amount ($E(4405 - 5495)$) and type (R_{5495}) of extinction and logarithmic distance ($\log d$) as variables. We used two alternative extinction law families: CCM (Cardelli et al. 1989) and new (Maíz Apellániz 2013a, Maíz Apellániz et al. 2014). For the fit we used the WFPC2 F336W + F439W + F487N + F502N + F547M + F656N + F673N + F675W + F814W and the 2MASS $J + H$ filters. The K_s -band photometry was excluded due to the IR excess caused

Table 2: The multiple system Herschel 36. The separations, positions angles, and magnitude differences are all with respect to A.

Component	Other name	Separation (")	PA (°)	$\Delta F814W$ (mag)
Ba	KS 1-S	2.913	8.7	6.98
Bb	KS 1-N	3.484	4.3	~ 14
C*	Herschel 36 SE	0.250	110.0	—
D	G5.97-1.17	2.903	123.3	6.40
E		0.740	201.7	4.82
F		4.196	125.8	10.0
G		2.774	272.6	10.3
H		2.415	112.0	10.4
I		3.456	168.2	12.3
J		1.660	313.0	~ 13

* Data from Goto et al. (2006).

by Herschel 36 C (see talk by J. Maíz Apellániz). The results are shown in Table 1 and Figure 4): the new extinction laws provide a better fit to the optical+NIR data, especially for F336W. It should be pointed out that the original CCM paper used Herschel 36 as an anchor point for large- R_{5495} extinction laws but they overestimated the amount of extinction ($E(B - V) = 0.89$) and underestimated R_{5495} (5.30).

7 Herschel 36: onto the UV

We compared the IUE spectroscopy with the F170W + F255W magnitudes (Figure 4). There is agreement between the IUE and WFPC2 fluxes a sign that the IUE extraction corresponds to the point source (it does not include the reflection nebula). There is a discontinuity between the CCM fit to the optical+NIR data and the IUE spectroscopy at the UV-optical boundary. On the other hand, there is an agreement with the large- R_{5495} extinction laws measured in 30 Doradus (Maíz Apellániz et al. 2014). We calculated the UV extinction law A_λ/A_{5495} by dividing the measured IUE flux by the intrinsic TLUSTY SED derived from CHORIZOS and the new extinction laws (Figure 5). We found that:

- The $R_{5495} = 5.0$ CCM law works better than the $R_{5495} = 5.3$ CCM law (the value used by CCM).
- The 2175 Å bump is weaker than in the CCM laws.
- The most likely explanation for the above is that CCM used the wrong value of $E(4405 - 5495)$.

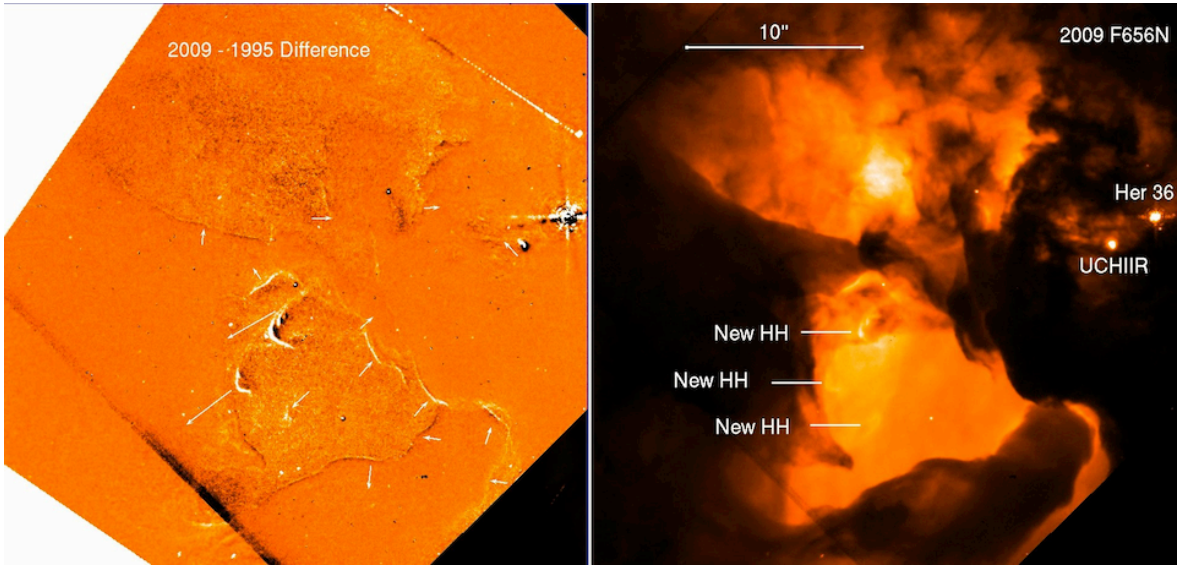


Figure 6: (left) Differential F656N image between 2009 and 1995. Whiter colours indicate stronger emission in 2009. The white arrows mark the direction of the detected movement. Their lengths are proportional to the modulus of the motion vectors. North is up and east is left. (right) F656N image of the same region. Herschel 36, the ultracompact H II region G5.97-1.17, and the newly discovered Herbig-Haro objects are labelled.

8 Other sources in the Hourglass

There is only a handful of point sources seen in most optical filters in the PC. We have measured the separations, position angles, and $\Delta F814W$ for the Herschel 36 multiple system (Table 2), defined as the objects within $5''$ of A: We have not attempted to resolve the embedded star Herschel 36 C (the contrast in the optical is very large and we are using aperture photometry), so the information provided in that case is from Goto et al. (2006). We note that Herschel 36 Ba is much brighter than Bb in F814W (Arias et al. 2006).

Probably, the most interesting component of Herschel 36 after A is D (\equiv G5.97-1.17), an ultracompact H II region proposed as a proplyd by Stecklum et al. (1998). For Herschel 36 D we measured a shift of ~ 0.3 PC px ($0''.015$ or 19 AU) between 1995 and 2009 (Figure 6): this might correspond to the orbital motion around Herschel 36 with a minimum period of 17 000 a. We also determined the extinction from the $H\alpha/H\beta$ ratio (F487N and F656N have low continuum contamination) assuming the same R_{5495} as for Herschel 36 A and obtained $A_{5495} = 9.9 \pm 0.3$ mag.

9 Herbig-Haro objects and nebular expansion

The comparison between new and archival WFPC2 images also reveals internal movements in the Hourglass Nebula. Three new Herbig-Haro objects are identified in Figure 6:

the HH nebular structures are displaced $0''.2$ - $0''.3$ during the interval between observations, indicating tangential velocities of 85-130 km/s. Also, a variety of nebular structures show displacements of up to 1 px ($0''.045$), suggesting an anisotropic expansion of the whole Hourglass Nebula (Figure 6).

References

- Arias, J. I. et al. 2006, *MNRAS* **366**, 739.
- Arias, J. I. et al. 2010, *ApJL* **710**, 30.
- Cardelli, J., Clayton, G. C., & Mathis, J. S. 1989, *ApJL* **345**, 245.
- Gilliland, R. L. 1994, *ApJL* **435**, 63.
- Goto, M. et al. 2006, *ApJ* **649**, 299.
- Maíz Apellániz, J. 2003, *2002 HST Calibration Workshop*, 346.
- Maíz Apellániz, J. 2004, *PASP* **116**, 859.
- Maíz Apellániz, J. 2013a, *Highlights of Spanish Astrophysics VII*, 583.
- Maíz Apellániz, J. 2013b, *Highlights of Spanish Astrophysics VII*, 657.
- Maíz Apellániz, J. et al. 2014, *A&A* **564**, 63.
- Sota, A. et al. 2014, *ApJS* **211**, 10.
- Stecklum, B. et al. 1998, *AJ* **115**, 767.